Effect of soil rigidity index and OCR on excess pore-water pressures generated around a piezocone penetrating in clay

Mohamad Reza Khodayari
Master of Geotechnical Engineering, Dept. of Civil Engineering, Sharif Univ. of Technology, Tehran, Iran. Email: khodayari.mhr@gmail.com

Mohammad Mehdi Ahmadi
Professor, Geotechnical Engineering Group, Dept. of Civil Engineering, Sharif Univ. of Technology, Tehran, Iran (Corresponding Author). Email: mmahmadi@sharif.edu

ABSTRACT: In this paper, piezocone penetration test (CPT*u*) in intact clays is numerically modeled via finite element formulation in which the soil is assumed to behave as modified Cam-clay law. Numerical results of CPT*u* modeling, e.g., tip resistance and generated excess pore-water pressure (EPWP) at u_1 and u_2 positions are compared to and validated with some experimental test results available in the literature. To consider the effect of in-situ stresses and overconsolidation ratio (OCR), the modeling is carried out under three different stress states and four distinctive stress histories. It is shown that EPWP distribution along the friction sleeve of a penetrating piezocone, starting from u_2 position, reasonably follows an exponential trend. Further investigations are performed to mention the soil parameters most influential on the afore-mentioned distribution trend. It is found that OCR and rigidity index (I_r) of the soil play important roles in the trends of EPWP generated along the friction sleeve.

Keywords: Piezocone penetration test (CPT*u*) in clay; Rigidity index (I_r); Overconsolidation ratio (OCR); Excess pore-water pressure; Finite element analysis.

1. Introduction

Piezocone penetration test (CPT*u*) is being widely used to characterize the properties of the soil under investigation, throughout the world. The CPT*u* is able to measure pore-water pressures along with the tip resistance (q_c) during the penetration. Measurements of pore-water pressures are usually limited to a number of sensors installed at specific locations on the device i.e. at the middle of the conical face (u_1); at the cone shoulder (u_2); and behind the friction sleeve (u_3) in some infrequent cases. The values of pore-water pressures measured at these locations are significantly affected by the properties of the soil under penetration. For example, Robertson et al. [1] showed that the distribution of excess pore-water pressures around the friction sleeve is heavily influenced by the soil OCR. Although separate use of the pore-water pressure measurements may be useful in correlating with soil characteristics, simultaneous assessment of them and identifying the parameters affecting their variations may better correlate the CPT*u* measurements to the soil properties.

The present study has the goal to investigate soil properties affecting the values of excess pore-water pressures (EPWPs) generated along the piezocone friction sleeve during the penetration, including Δu_2 (= $u_2 - u_o$) and Δu_3, where u_o = hydrostatic pore-water pressure. The investigation is based on FE modeling of undrained piezocone penetration test in intact clayey soils, in which the generated EPWPs are positive i.e. $\Delta u > 0$ [2]. Considering different properties and various stress states for the soil, in the numerical modeling, the most influential soil parameters are identified to be as OCR and rigidity index (I_r). According to the obtained results, the values of $\Delta u_3/\Delta u_2$ tend to decrease with increasing OCR and to decrease with decreasing the rigidity index of the soil.

2. Numerical analysis

Piezocone penetration test in fully saturated intact clays under undrained conditions is numerically modeled via non-linear FEM in axisymmetric mode using software package Abaqus 6.14-4 [3].

2.1. Modeling

The model simulates a calibration chamber configuration (i.e. uniform initial stress state) with different presumed vertical effective stresses of 18, 45 and 90 kPa applied separately as the surcharge at the top surface and K_o conditions. This configuration, in fact, predicts the CPT*u* measurements at a specified depth in the soil profile.

Implicit scheme is used to model the penetration process of the standard piezocone with 60° apex angle and 1000 mm^2 base cross-sectional area as an impermeable rigid body in a coupled pore fluid-stress mode of analysis (consolidation analysis). In order to simultaneously handle the soil boundary condition effects and computational time cost, the dimensions of the soil body, in the numerical model, is considered to be as 65r and 45r in the vertical and radial directions, respectively; where r = radius of the piezocone (= 17.84 mm). The soil body is discretized using 8-noded quadratic axisymmetric rectangular elements (CAX8RP) with a constant height of 0.4r from top to bottom and a linearly varied radial size of 0.4r adjacent the axis of symmetry to 2r at the right boundary of the soil body. Fig. 1 represent the schematic dimensions of the model domain. The conical face of the piezocone is modeled buried in soil domain to overcome the excessive distortions of the soil elements at the beginning of t-

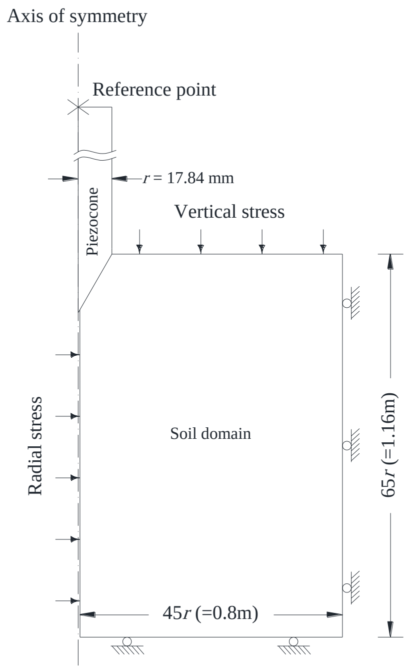

Figure 1. Schematic geometry and mesh of the FE model

he penetration. In order to permit soil elements to flow around the penetrating piezocone, left boundary of the soil body is offset at a value of $0.05r$ from the axis of symmetry as proposed by Ahmadi et al. [4] and Yi et al. [5]. The right and bottom sides of the soil body are bounded in radial and vertical directions, respectively; and uniform radial and vertical stresses are applied to the left and top surfaces, respectively. Initial radial and hoop stresses are assumed to be equal. The value of coefficient of earth pressure at rest (K_o) is expressed in terms of soil effective friction angle (ϕ') and OCR [6] as

$$K_o = \left(1 - \sin\phi'\right) \mathrm{OCR}^{\sin\phi'} \tag{1}$$

The movements of the rigid piezocone is controlled by a reference point subjected above its central line of mass symmetry. Thus, the penetration process is performed by applying a standard downward velocity of 20 mm/s to the reference point. The reference point is also shown in Fig. 1 as well as axis of symmetry, boundary constraints, and applied radial and vertical stresses. According to ASTM-D5778 [7] specifications, pore-water pressures at u_2 and u_3 are read at a distance of 3 mm above the cone base and 134 mm above the u_2 position, respectively; in the numerical model. Surface to surface master-slave kinematic contact algorithm is used to model the interaction between the soil and piezocone. In this type of formulation the master surface can only penetrate in slave surface. Therefore, slave and master surfaces are dedicated to soil and piezocone, respectively; due to the physical phenomena that it is the advancing cone that pushes the soil particles aside and soil particles cannot penetrate into the solid cone. Hard normal contact, which is responsible for pressure transmission prevention when the two surfaces are not in contact, is used to model the normal contact behavior between the two surfaces. If the type of contact is compressive, the contact will remain intact; however, if it is tensile, no interaction between the two surfaces happens and the tensile stresses automatically become zero. This is due to the fact that tensile stresses cannot be generated between the two surfaces of piezocone and soil. The maximum magnitude of shear stress transmitted between the master and slave surfaces is limited to the soil adhesion. Coulomb friction law is used in this study to control the finite sliding between the two surfaces by use of a frictional coefficient and limiting the induced shear stresses to the soil adhesion.

The stress-strain behavior of the soil material is described by Modified Cam-clay (MCC) model. Input parameters of this model include slope of the swelling line (κ); slope of normal compression line (λ); void ratio at $p' = 1$ kPa on normal compression line (e_N) or initial void ratio (e_o); where all these parameters are defined in e-lnp' space (e = void ratio and p' = mean effective stress); and slope of critical state line (M) which is defined in q-p' space, where q = deviatoric stress. The shear modulus (G) of a MCC soil is considered to depend on the mean effective stress with a constant poisson's ratio (υ). Considering K_o-consolidated triaxial compression (CK_oUC) mode for estimating the undrained shear strength (s_u) from MCC parameters [8, 9], the rigidity index ($I_r = G/s_u$) can be expressed as

$$I_r = \frac{\left(3 - 6\upsilon\right)\left(1 + e\right)}{M\left(1 + \upsilon\right)\kappa}\left(\frac{R}{2}\right)^{\frac{\kappa - \lambda}{\lambda}} \tag{2}$$

where R = isotropic OCR; $M = 6\sin\phi'/(3 - \sin\phi')$; and e = current void ratio obtained from standard relationships in e-lnp' space [10] for each case of study, based on current stress state of the soil. The hydraulic conductivity is assumed to be isotropic for simplicity.

In order to conduct a comprehensive investigation, a number of different cohesive soils with a wide range of MCC parameters is utilized in this study as shown in Table 1. Poisson's ratio (υ) is considered to be 0.3 for all cases of analysis except for Woodberry clay which was reported to be 0.333. In order to consider the effect of different stress histories, each aforementioned presuming vertical effective stresses, i.e. 18, 45 and 90 kPa, are analyzed under four distinctive presuming practical OCRs of 1, 3, 6 and 10. Values of R is adjusted for anisotropic soil conditions using the relationships given by Chang et al. [8]; and implementation of various convetional OCRs is handled by changing the size of initial yield surface and adjusting the value of radial effective stress using Eq. (1).

2.2. Validation

The proposed numerical modeling procedure has proved to provide a reliable framework of well predicting the CPT*u* measurements in intact clayey soils. Here, the results of numerical simulation of laboratory calibration chamber tests performed by Kurup et al. [11] and Lim [12] on K-50 (50% kaolinite + 50% fine sand by weight) and K-33 (33% kaolinite + 67% fine sand by weight) soil samples, respectively, are compared with the laboratory test measurements and illustrated in Fig. 2. The dash lines in this figure represent ±15% error compared to the measured values. The model parameters used for K-50 and K-33 are taken from Abu-Farsakh et al. [13] and include:

Table 1. Modified Cam-clay model parameters for soils utilized in numerical modeling

Soil	κ	λ	M	e_N	ϕ' (°)	k † (m/s)	Reference
Kaolin clay	0.044	0.205	0.92	2.252	23	1.02×10^{-09}	Mahmoodzadeh and Randolph [14]
Woodberry clay	0.03	0.126	1.33	2.144	33	3.76×10^{-09}	Ansari et al. [15]
K-50	0.024	0.11	1.2	1.222	30	5.00×10^{-10}	Abu-Farsakh et al. [13]
Boston blue clay	0.034	0.184	1.348	1.967	33.4	5.00×10^{-10}	Whittle et al. [16]
Bothkennar	0.03	0.365	1.42	2.850	35	1.00×10^{-10}	Lehane and Jardine [17]
Gault clay	0.035	0.219	1.0	3.088	25.4	9.37×10^{-10}	Wood [10]
Kaolin clay 2	0.05	0.25	0.9	2.699	23	2.55×10^{-09}	Wood [10]
Weald clay	0.031	0.088	0.882	1.097	22.6	1.27×10^{-12}	Carter [18]
London clay	0.062	0.161	0.888	1.752	23	1.00×10^{-10}	Schofield and Wroth [19]

†Coefficient of permeability

Table 2. Measurements of chamber tests performed by Kurup et al.† [11] and Lim‡ [12]

Soil Material	σ'_{vo} (kPa)	σ'_{ho} (kPa)	OCR	Measured $u_1 - u_o$ (kPa)	Measured $u_2 - u_o$ (kPa)	Measured $q_t - u_o$ (MPa)
K-50†	207	207	1	562	624	1.20
K-50†	41.4	41.4	5	528	406	0.60
K-50†	207	107.6	1	490	368	0.67
K-33‡	207	207	1	649	620	1.45
K-33‡	262.2	262.2	1	794	779	1.80
K-33‡	24.2	40.7	10.9	308	266	1.03

$\kappa = 0.024$; $\lambda = 0.11$; $M = 1.2$; $e_o = 1.0$ for K-50; and $\kappa = 0.01$; $\lambda = 0.06$; $M = 1.0$; $e_o = 1.0$ for K-33. To have an appropriate comparison, another mesh with the same size as the chamber and piezocone used by Kurup et al. [11] and Lim [12] is modeled in this study. It is noted that, modeling procedure was the same as what is explained in the previous sub-section, and the only difference is in model dimensions and mesh size. Test data for calibration chamber tests are provided in Table 2. In this table, σ'_{vo} and σ'_{ho} are initial vertical and horizontal effective stresses, repectiv-ely, and q_t is corrected tip resistance. Notably, according to Fig. 2, the numerically predicted values of pore-water pressure and tip resistance compare generally well with the experimental measurements.

3. Results

Penetration process, in the numerical modeling, is continued until the conical face of the piezocone reaches the mid-height of the soil domain (i.e. 580 mm of penetration). Penetration resistance profile for a simulated case is illustrated in Fig. 3. As shown in Fig. 3, the value of tip resistance reaches a steady state as the penetration continues. This is because of the calibration chamber configuration considered in the modeling (i.e. constant initial stresses). The final constant values are considered as the results of numerical simulation for the specified depth of the soil with specified parameters and stress state. According to the numerical results, the value of permeability coefficient (k) has a significant effect on the values of generated EPWPs around the advancing piezocone. Parametric studies performed on the permeability coefficient in this study showed that a value of $k = 3.0 \times 10^{-9}$ m/s may be regarded as the boundary of undrained condition of penetration in the presumed OCR range of 1 to 10. In other words, permeability coefficients about the aforementioned value (3.0×10^{-9} m/s) and lower lead to obtain identical values of generated EPWPs (i.e. undrained condition of penetration). Most of the clayey soils encountered in practice, including the ones listed in Table 1, usually represent permeability coefficients about $k = 3.0 \times 10^{-9}$ m/s or lower [20]. Thus, this study covers

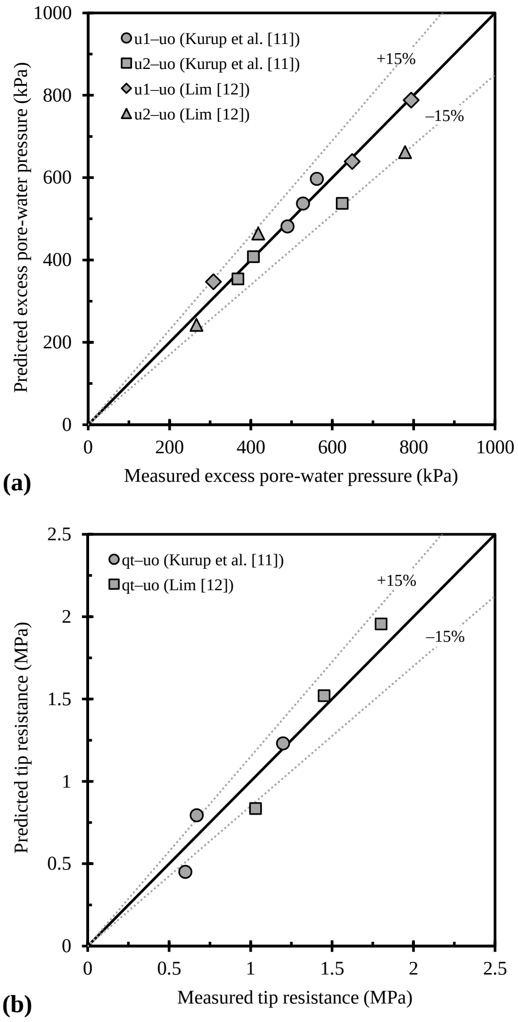

Figure 2. Comparison of calibration chamber test measurements with associated numerical simulation results of this study; (a) Excess pore-water pressure, and (b) Tip resistance

undrained standard piezocone penetrations which are generally representative of the cases encountered in practice as well. Of course, there are other cases in practice in which penetration can be considered partially drained or drained. The criteria for these conditions depend on soil permeability in standard piezocone penetrations [21]. In this study the permeability is considered to be low enough so that only undrained penetrations can be accepted.

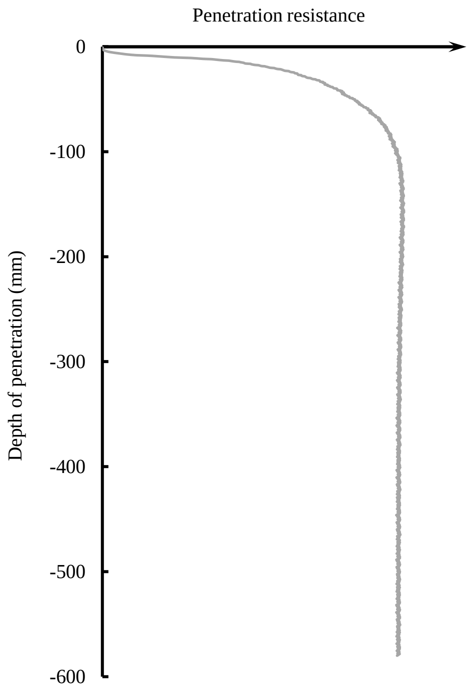

Figure 3. Profile of penetration resistance, obtained from the numerical simulation

3.1. Distribution of excess pore-water pressures

In order to study the EPWP distribution along the friction sleeve, in addition to the readings of Δu_2 and Δu_3, values of generated EPWPs are read at the elemental nodes between u_2 and u_3 adjacent the piezocone shaft. Fig. 4 illustrates the EPWPs generated along the friction sleeve for all soil cases listed in Table 1 at σ'_{vo} = 45 kPa with various OCRs of 1, 3, 6 and 10. In Fig. 4, z = upward distance of any point from u_2 position adjacent and along the friction sleeve (a number between zero and 0.134 m), and Δu_z = EPWP associated with that point. Values of rigidity index (I_r) and OCR are also presented in Fig. 4 for each case of study. Refering to Fig. 4, it is observed that the trends of EPWP generated along the friction sleeve vary significantly with I_r and OCR. The difference between Δu_3 and Δu_2 values tends to become larger with increasing OCR and decreasing I_r. Consequently, the value of $\Delta u_3/\Delta u_2$ tends to decrease with increasing OCR and decreasing I_r. Such a change in $\Delta u_3/\Delta u_2$ with regards to OCR is also reported by Robertson et al. [1] based on field measurements.

Several trends are tried in this study to represent the EPWP distributions illustrated in Fig.4, and it is concluded that exponential trends can best fit the obtained numerical results. Fig. 5 shows four exponential curves fitted on the results obtained for the case of Kaolin clay (Table 1) at σ'_{vo} = 45 kPa, as an example; where the formula of each trend is also provided in Fig. 5.

Separate effect of OCR and soil rigidity index (I_r) has been investigated in this study and presented in the following sections. In the case of effect of OCR on the generated EPWPs around the piezocone, four numerical analyses with four various OCRs are carried out under a constant value of rigidity index. Next, for evaluation of effect of rigidity index separately, eight additional analyses are performed considering constant OCRs with different rigidity index values.

3.2. Effect of soil OCR

Assessment of separate effect of OCR on generated E-PWPs along the friction sleeve has been carried out using four different OCR values of 1, 3, 6 and 10 but with a constant value of rigidity index. This has been performed by choosing various MCC soil parameters which result in obtaining identical rigidity index based on Eq. (2) while the OCR is different. According to Eq. (2), by taking constant values for M, υ and λ, it is possible to obtain an identical value for I_r, just by adjusting the value of isotropic OCR (R) and slope of the swelling line in e-lnp' space (κ). The value of λ is assumed to be five times the value of κ for each case of study in this section. Table 3 represents the MCC parameters analyzed for the cases in this section. A constant value of I_r = 55 is obtained for all cases listed in Table 3, based on the associated MCC parameters and overconsolidation ratios. The analyses are performed at σ'_{vo} = 45 kPa with assumed values of e_N = 2.8, υ = 0.3, M = 1.0 and K_o values varying wih OCR.

Table 3. MCC soil parameters used for assessing the effect of OCR at a constant value of I_r (σ'_{vo} = 45 kPa; e_N = 2.8; and υ = 0.3)

Case	λ	κ	M	OCR	K_o	I_r
MCC1	0.325	0.065	1.0	1	0.6	55
MCC2	0.175	0.035	1.0	3	0.9	55
MCC3	0.125	0.025	1.0	6	1.2	55
MCC4	0.100	0.020	1.0	10	1.5	55

Fig. 6 represents the results of EPWP trends obtained for soil cases of MCC1-MCC4 (Table 3). According to Fig. 6, the values of $\Delta u_z/\Delta u_2$ tend to decrease with increasing OCR at a constant value of I_r.

3.3. Effect of soil rigidity index

Similar to the previous section, separate effect of I_r is investigated by choosing MCC soil parameters which lead to obtain different I_r values while having identical values of OCR. For each assumed OCR (1, 3, 6 and 10) the MCC parameters are chosen in a way that two different values of I_r is obtained for each of aforementioned OCR values. Table 4 shows the MCC parameters used for simulations in this section. K_o is varied with OCR and values of M, e_N and υ are considered to be constant and equal to 1.0, 2.8 and 0.3, respectively. In addition, the value of λ is assumed to be five times the value of κ. The analyses are carried out at σ'_{vo} = 45 kPa.

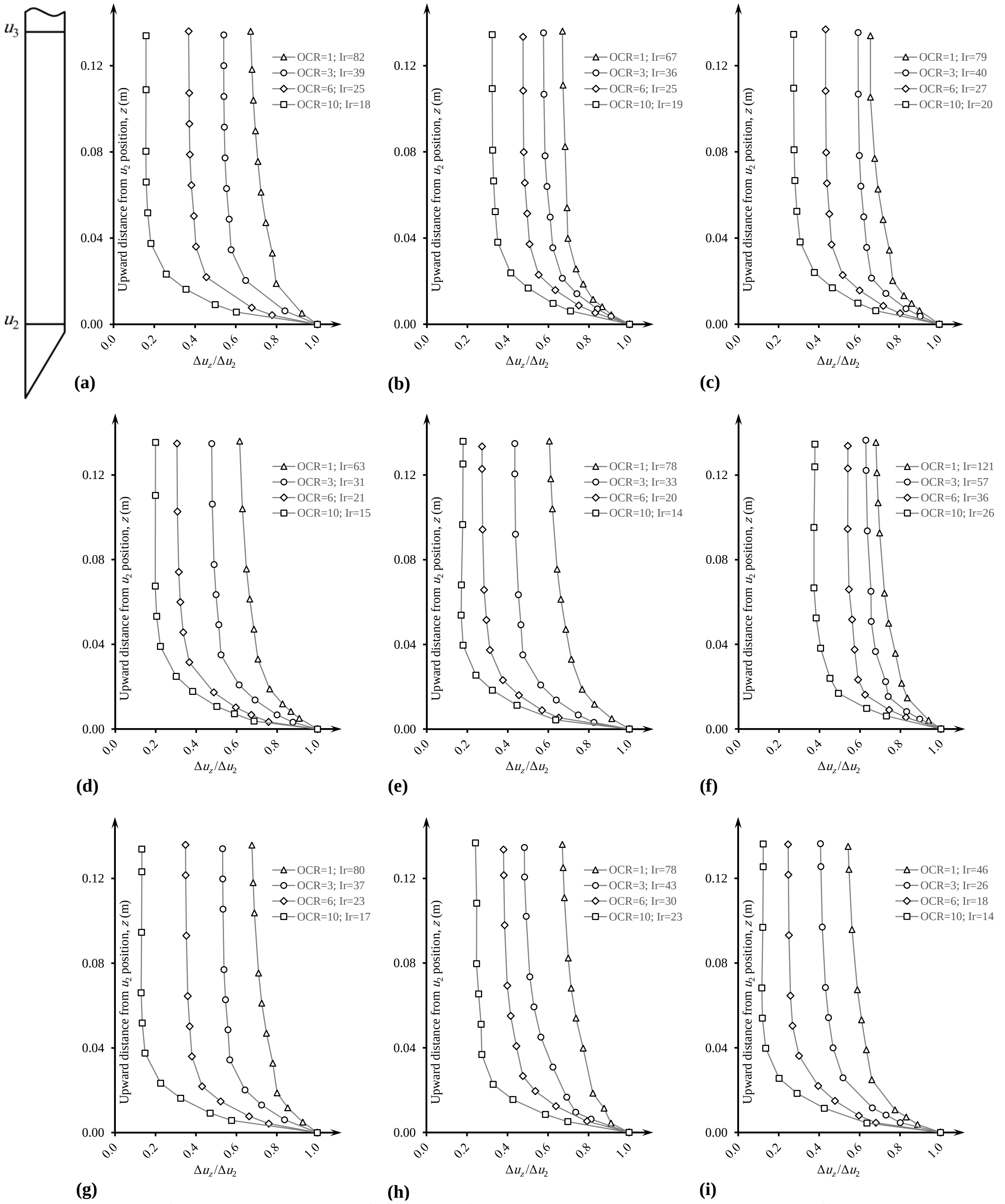

Figure 4. Distribution of generated EPWPs along the friction sleeve for all cases listed in Table 1, at σ'_{vo} = 45 kPa with different OCRs and I_r values; for (a) Kaolin clay, (b) Woodberry clay, (c) K-50, (d) Boston blue clay, (e) Bothkennar, (f) Gault clay, (g) Kaolin clay 2, (h) Weald clay, (i) London clay

According to Table 4, different soils with same values of OCR can take different values of I_r. Based on numerical results, this issue has caused different soils with the same OCR to have different trends of EPWP around the piezocone. Fig. 7 shows the EPWP trends along the friction sleeve for soil cases of MCC5-MCC12 listed in Table 4. According to Fig. 7, different I_r values result the EPWP trends to differ even in constant OCRs.

4. Conclusion

Undrained piezocone penetration test in fully saturated intact clay is numerically simulated via FEM in this study in order to investigate and identify the most influential soil parameters on the distribution trends of excess pore-water pressure (EPWP) generated along the friction sleeve. A relatively wide range of Modified Cam-clay m-

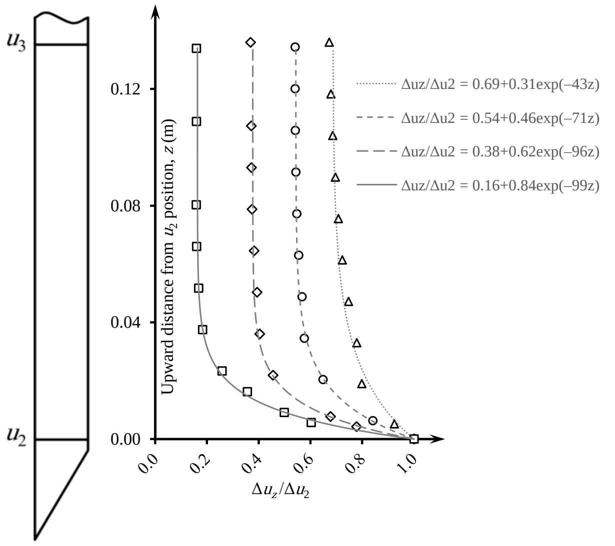

Figure 5. Exponential fitted curves on numerical results

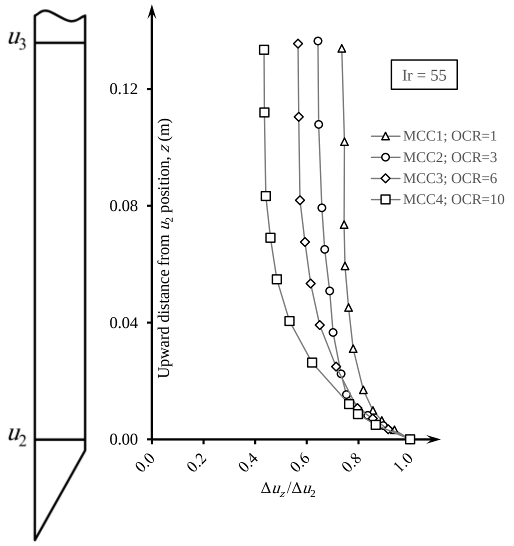

Figure 6. Separate effect of OCR on EPWP trends along the friction sleeve

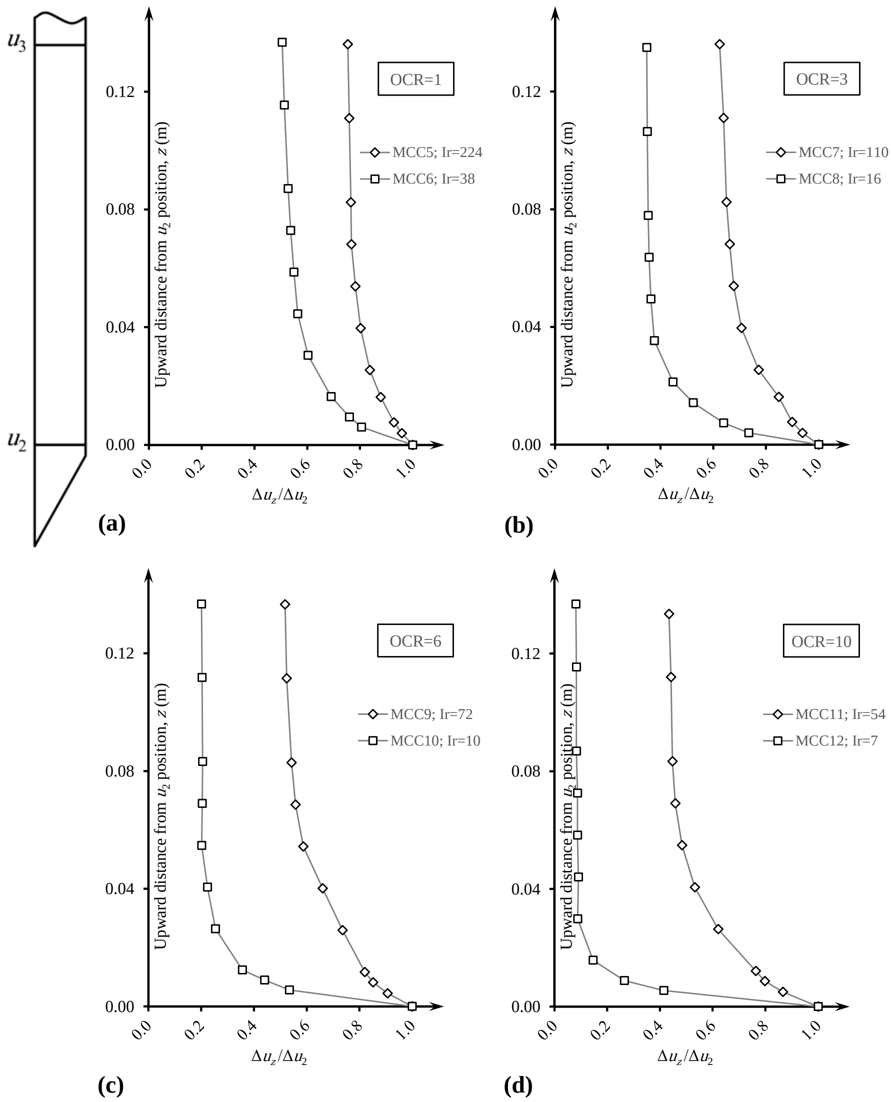

Figure 7. Separate effect of I_r on EPWP trends along the friction sleeve at four different overconsolidation ratios of (a) OCR=1, (b) OCR=3, (c) OCR=6 and (d) OCR=10

Table 4. MCC soil parameters used for assessing the effect of I_r at four different OCRs (σ'_{vo} = 45 kPa; e_N = 2.8; and υ = 0.3)

Case	λ	κ	M	OCR	K_o	I_r
MCC5	0.10	0.02	1.0	1	0.6	224
MCC6	0.40	0.08	1.0	1	0.6	38
MCC7	0.10	0.02	1.0	3	0.9	110
MCC8	0.40	0.08	1.0	3	0.9	16
MCC9	0.10	0.02	1.0	6	1.2	72
MCC10	0.40	0.08	1.0	6	1.2	10
MCC11	0.10	0.02	1.0	10	1.5	54
MCC12	0.40	0.08	1.0	10	1.5	7

odel parameters for clayey soils throughout the world are investigated in this study and it is found that the generated EPWP trend along the piezocone shaft follows an exponential trend which is heavily affected by rigidity index (I_r) and overconsolidation ratio (OCR) of the soil. Further parametric investigations are performed to mention the separate effect of each parameters of I_r and OCR on the aforementioned trend. It is shown that the values of generated EPWPs along the friction sleeve of a penetrating piezocone tend to decrease with increasing OCR, and to decrease with decreasing I_r.

References

[1] Robertson, P. K., Campanella, R. G., Gillespie, D., Greig, J. "Use of piezometer cone data", In *Use of in situ tests in geotechnical engineering*, 1986, pp. 1263–1280.

[2] Ouyang, Z., Mayne, P. W. "Effective friction angle of clays and silts from piezocone penetration tests", *Canadian Geotechnical Journal*, vol. 55, no. 9, pp. 1230–1247, 2017.

[3] Dassault Systèmes. (2014). Abaqus version 6.14-4 documentation. Dassault Systems Simulia Corporation.

[4] Ahmadi, M. M., Byrne, P. M., Campanella, R. G. "Cone tip resistance in sand: modeling, verification, and applications", *Canadian Geotechnical Journal*, vol. 42, no. 4, pp. 977–993, 2005.

[5] Yi, J. T., Goh, S. H., Lee, F. H., Randolph, M. F. "A numerical study of cone penetration in fine-grained soils allowing for consolidation effects", *Géotechnique*, vol. 62, no. 8, p. 707, 2012.

[6] Mayne, P. W., Kulhawy, F. H. "Ko- OCR Relationships in Soil", *Journal of the Soil Mechanics and Foundation Division*, vol. 108, no. 6, pp. 851–872, 1982.

[7] ASTM-D5778-12, *"Standard Test Method for Electronic Friction Cone and Piezocone Penetration Testing of Soils"*, vol. 4, pp. 1587–1605, 2012.

[8] Chang, M., Teh, C., Cao, L. "Critical state strength parameters of saturated clays from the modified Cam clay model", *Canadian Geotechnical Journal*, vol. 36, no. 5, pp. 876–890, 1999.

[9] Wroth, C. P. "Interpretation of in situ soil tests", *Geotechnique*, vol. 34, no. 4, pp. 449–489, 1984.

[10] Wood, D. M. "*Soil behaviour and critical state soil mechanics"*, Cambridge university press, 1990.

[11] Kurup, P. U., Voyiadjis, G. Z., Tumay, M. T. "Calibration chamber studies of piezocone test in cohesive soils", *Journal of Geotechnical Engineering*, vol. 120, no. 1, pp. 81–107, 1994.

[12] Lim, B. "Determination of Consolidation Characteristics in Fine Soils Evaluated by Piezocone Tests", PhD Thesis, Louisiana State University, 1999.

[13] Abu-Farsakh, M., Tumay, M., Voyiadjis, G. "Numerical parametric study of piezocone penetration test in clays", *International Journal of Geomechanics*, vol. 3, no. 2, pp. 170–181, 2003.

[14] Mahmoodzadeh, H., Randolph, M. F. "Penetrometer testing: effect of partial consolidation on subsequent dissipation response", *Journal of Geotechnical and Geoenvironmental Engineering*, vol. 140, no. 6, p. 4014022, 2014.

[15] Ansari, Y., Merifield, R., Sheng, D. "A piezocone dissipation test interpretation method for hydraulic conductivity of soft clays", *Soils and Foundation*, vol. 54, no. 6, pp. 1104–1116, 2014.

[16] Whittle, A. J., DeGroot, D. J., Ladd, C. C., Seah, T.-H. "Model prediction of anisotropic behavior of Boston Blue Clay", *Journal of Geotechnical Engineering*, vol. 120, no. 1, pp. 199–224, 1994.

[17] Lehane, B., Jardine, R. J. "The behaviour of a displacement pile in Bothkennar clay", In *Predictive soil mechanics. Proceedings of the Wroth Memorial Symposium,* St Catherine's College, OXFORD, 1993.

[18] Carter, J. P. "Predictions of the non-homogeneous behaviour of clay in the triaxial test", *Geotechnique*, vol. 32, no. 1, 1982.

[19] Schofield, A., Wroth, P. "*Critical state soil mechanics"*, vol. 310. McGraw-Hill London, 1968.

[20] Look, B. G. "*Handbook of geotechnical investigation and design tables"*, CRC Press, 2014.

[21] [Khodayari, M. R., Ahmadi, M. M.]. Forthcoming. "[Excess pore-water pressure along the friction sleeve of a piezocone penetrating in clay: A numerical study]." [*International Journal of Geomechanics*]. [10.1061/(ASCE)GM.1943-5622.0001702].